In silico Homology Modeling and Docking Studies of RecA from *Campylobacter jejuni*

Mohammed Zaghlool Al-Khayyat

Department of Biology, College of Education for Pure Sciences
University of Mosul, Mosul City, Iraq
E-mail: mzsaeed19@hotmail.com

Received: April 03, 2017 **Accepted: December 15, 2018**

Published: March 30, 2019

Abstract: *The RecA protein has an essential role in DNA recombination and repair which is mediated by its ability to bind ATP/ADP. SWISS-MODEL, an online automated server, was used to predict its tertiary structure of C. jejuni RecA. Four evaluation tools were used for quality assessment of the constructed model: QMEAN6, ERRAT, ANOLEA and PROCHECK. Quality assessments indicated that the model was of high quality and reliable for docking experiments. A total of forty natural products were used in docking the model by Hex 8.0.0 and ArgusLab 4.0.1 using ADP as control. Ten compounds had docking scores higher than that of ADP (-8.61 Kcal/mol) in ArgusLab 4.0.1 where quercetin had the highest docking score of -10.34 Kcal/mol. In Hex 8.0.0 docking, only cucurmin, taxifolin, isoquercitrin and vitexin had docking scores higher than that of ADP. These natural occurring compounds may be possible inhibitors of ATPase activity and, therefore, may be further analyzed to develop new antimicrobials targeting RecA in pathogenic bacteria.*

Keywords: *Antibiotic design, ArgusLab, Cucurmin, Homology modeling, Taxifolin, Quercetin.*

Introduction

The RecA protein is involved in DNA recombination and repair of prokaryotes and eukaryotes. In DNA recombination, RecA can displace a single-stranded DNA from its homolog and promote the exchange of the complementary strands between double helices in a process called single stand assimilation. In DNA repair, the SOS response is induced when RecA inactivates LexA, a repressor of 40 genes (e.g., *RecA, lexI, uvrA, uvrB, uvrC*) that are involved in repairing DNA damage [12, 35]. The SOS and recombination processes have been shown to be activated in response to antibiotic treatment, therefore, RecA is likely to be involved in the development and transfer of antibiotic resistance. These functions are achieved by binding ADP/ATP molecules [4, 21].

Protein-ligand docking is carried out by various bioinformatic tools; however, these tools use different scoring systems and methods in estimating the binding affinities of protein targets with ligands. Hex 8.0.0 is a molecular graphic program which uses spherical polar Fourier correlations to accelerate calculations. It is used to determine docking modes of DNA and proteins and can also used for estimating protein-ligand binding [33]. Modi et al. [28] conducted a docking study of anti-HIV drug derivatives using Hex 6.3 against GP120, a viral protein.

ArgusLab has become a favorite tool for researchers because it is easy to work with and free. This docking engine approximates an exhaustive search method where flexible ligand docking is achieved. The ligand is considered as a torsion tree and grids are made up to cover the binding site of the receptor. The ligand root node, which is the unbounded group of atoms with no rotatable bonds, is placed in a search point inside the binding site and a set of diverse

and energetically favored rotations is developed. For each rotation, those poses that survive torsion search are scored. The N lowest energy poses (50-150) are retained where a final set of 25 poses undergo energy minimization and ranking [11].

Flavonoids are polyphenolic compounds produced by plants as secondary metabolites with many pharmacologic properties. Using ArgusLab, nine bioactive flavonoids and alkaloids were screened against a human DEK proto-oncogene to obtain a candidate compounds to act as anti-cancer agents, their binding affinities were in the range of (-5.91 to -8.65) Kcal/mol [38]. Balajee and Rajan [3] used ArgusLab in docking pantothenate synthase of *Mycobacterium tuberculosis* against ligands obtained from Chemspider database in order to identify an anti-tuberculosis agents where the best ligand had a binding energy of -12.22 Kcal/mol. Pathogenic bacteria have developed resistance to almost all antibiotics as a result of the widespread unwise use of currently available antibiotics [15]. Thus, the aim of this study is to build a 3D model of *C. jejuni* RecA which may be used in docking experiments that are selected to screen for novel inhibitors.

Materials and methods

Sequence retrieval, primary and secondary structure

RecA of *Campylobacter jejuni* subsp. jejuni NCTC 11168 was downloaded from NCBI available at http://www.ncbi.nlm.nih.gov/. NCBI Reference is CAL35769.1. The secondary structure was predicted by SSpro8 of SCRATCH at http://scratch. proteomics.ics.uci.edu/ [10]. The elements of secondary structure were determined according to Kabsch and Sander [19] as alpha-helix, 3-10-helix, extended strand, turn, bend, bridges, and the rest. The ATP/ADP binding site was predicted using FunFold at (www.reading.ac.uk.bioinf.servlets.NFOLD/FunFO LD2/) [34].

Homology modeling and evaluation of models

The protein tertiary structure of *C. jejuni* was built by an online server, SWISS-MODEL (http://swissmodel.Expasy.org/) [2] using a related template from Protein data bank, 3.15 Å X-ray crystallographic structure of RecA, PDB ID: 3cmtA [9] with a sequence identity of 64.36%, modeled residues were 36-324, and e-value 4.39724e-103. The model was evaluated to assess its quality. Overall quality of the model is estimated by ERRAT (http://services.mbi.ucla.edu/ERRAT/) [12]. The SWISS-MODEL workspace [2] (http://swissmodel.Expasy.org/workspace/) contains several evaluation tools, three of them were used (a) QMEAN6 server (Qualitative Model Energy ANalysis) [6], (b) PROCHECK, measures stereochemical properties [23], and (c) Analysis of Non-Local Environment of Atoms (ANOLEA) [27]. The model was submitted into Protein Model Data Base, available at http://bioinformatics.cineca.it/PMDB [8].

Molecular docking

Forty flavonoids were used in screening for RecA binding at its ADP-binding motif, using ADP as control. These compounds were downloaded from ZINC database (http://zinc.docking.org/) [18]. Rigid protein-ligand docking was performed on these structures by Hex 8.0.0 [38]. The settings were: Grid dimension = 0.6, docking solutions = 100, an initial steric scan at N = 16, followed by a final search at N = 26, receptor and ligand range 180 degrees. The docking software, ArgusLab 4.0.1 is available at http://www.arguslab.com/ and uses Ascore as an empirical scoring function whose terms were derived from Xscore [40, 44]. Flexible docking parameters were a grid center of 24.0, 24.0 and 24.0 for x, y and z respectively, grid resolution 0.40 and 150 evaluations.

Results and discussion

Fig. 1 shows the amino acid sequence and the secondary structure of RecA. SWISS-MODEL was used to predict a three dimensional model of *C. jejuni* RecA (Fig. 2). Four validation tools were used to check the quality of this model. ERRAT and ANOLEA depend on the thermodynamic hypothesis that the native protein is at the minimum energy state under normal conditions [24]. ERRAT (Fig. 3A) analysis shows that the model produced by SWISS-MODEL had an overall quality of 95.4%. ERRAT is a statistical potential used to detect regions of errors on the basis of heavy atomic-pair distributions (CC, CN, CO, NN, NO, OO). These statistics are compared with a set of 96 experimental structures. High resolution experimental structures usually produces quality factors of 95% or higher but for lower resolution structures a quality of 91% is accepted [23]. In ANOLEA (Fig. 3B) the produced model of *C. jejuni* had few high energy zones since their presence may suggest problems in the protein fold [27].

```
1   MDDNKRKSLDAALKSLDKTFGKGTILRLGDKEVEQIDSIGTGSVGLDLALGIGGVPKGRIIEIYGPESSGK
    CCHHHHHHHHHHHHHHHHHHCTTESCCTTCCCCCCCCEECCSCHHHHHHTSSSSEETTSEEEEEESTTSSH

72  TTLTLHIIAECQKAGGVCAFIDAEHALDVKYAKNLGVNTDDLYVSQPDFGEQALEIVETIARSGAVDLIVV
    HHHHHHHHHHHHHTTCCEEEEESSCCCCHHHHHHHTCCCGGCEEECCSSHHHHHHHHHHHHHTSCCSEEEE

143 DSVAALTPKAEIEGDMGDQHVGLQARLMSQALRKLTGIVHKMNTTVIFINQIRMKIGAMGYGTPETTTGGN
    ECETTCCCHHHHTSCCTSSSCHHHHHHHHHHHHHHHHHHHHHTCEEEEEEECECCSSSCCCCCSSSSSHHH

214 ALKFYASVRLDVRKVATLKQNEEPIGNRVKVKVVKNKVAPPFRQAEFDVMFGEGLSREGELIDYGVKLDIV
    HHHHHCSEEEEEEEEEECCSSSSCSEEEEEEEEEEESSSCCTCEEEEEEETTTEECHHHHHHHHHTTSSS

285 DKSGAWFSYKDKKLGQGRENSKAFLKENPEIADEITKAIQNSMGIEGMISGSEDDEGEE
    EESSSEEEETTEEEEESHHHHHHHHHHCHHHHHHHHHHHHHHTCCCCCCCCCCTTCTCC
```

Fig. 1 The amino acid sequence of C. jejuni RecA and its secondary structure as predicted by SSpro8 where H: alpha-helix, G: 3-10-helix, E: extended strand, T: turn, S: bend, C: the rest.

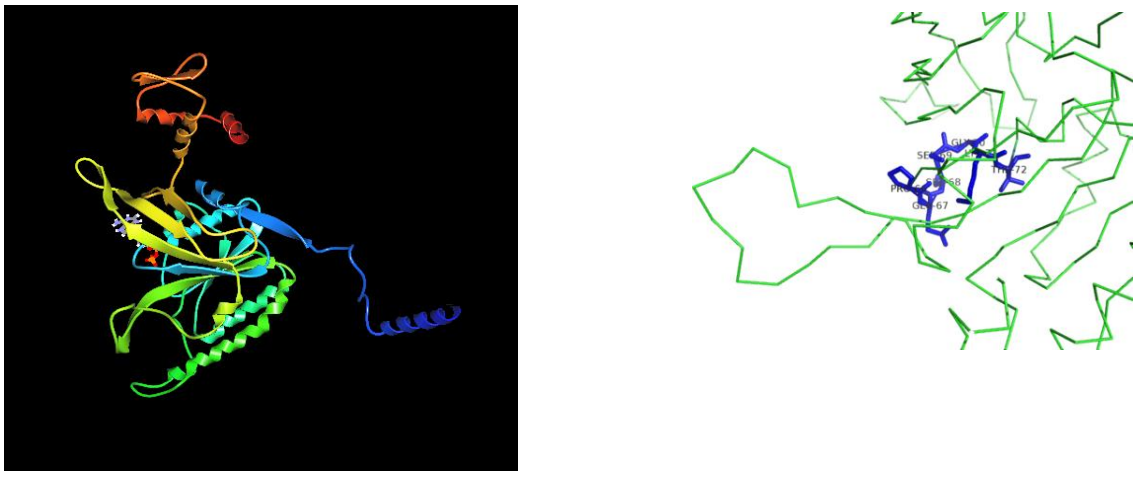

A) B)

Fig. 2 A) Three dimension structure of *C. jejuni* RecA generated by SWISS-MODEL; B) Binding cavity of ADP (blue in color) was predicted by FunFOLD and appears to extend from Pro^{66} to Thr^{72}.

C. jejuni RecA model had a QMEAN6 value of 0.6. QMEAN6 is another validation tool to select the native structure out of several predicted ones. QMEAN6 scores lie normally in the range of 0-1 for accurate reliable models. The measured parameters are: (a) the solvation potential to calculate the residues burial; (b) the torsion angle potential estimates the local amino acid geometry of the constructed model; (c) two distance-dependent potentials, one is based on β-atoms and the second is on all-atom potential as a measure of atomic interactions; and (d) two terms to compare the predicted secondary structure with a computed one (SSE agree.), and the solvent accessibility (ACC agree.) [5, 6]. A comparison of Z-scores with experimentally determined structures is shown in (Fig. 3C).

Ramachandran plot analysis of dihedral angles was one of the methods to differentiate allowed and non-allowed geometry of amino acid residues in a protein [31]. Laskowski et al. [23] suggested that a reliable model should have a Ramachandran plot in which more than 90% of the residues lie in the most favored region. SWISS-MODEL produced a model having a such value. Fig. 4 shows the Ramachandran plot of model. The model had 252 (90.3%) of residues in the most favored region, 24 (8.6%) residues in the additionally allowed region, 1 (0.4%) residue in generously allowed region, and 2 (0.7%) residues in disallowed region. Tables 1A and 2B represent the main and side chain parameters of the model as estimated by PROCHECK. Based on the above assessment, *C. jejuni* RecA model is considered reliable for use in docking. It was successfully submitted into the Protein Model Data Base and acquired PMDB ID: PM0080213.

Table 1A. Summary of the main-chain parameters of SWISS-MODEL in Ramachandran plot

Stereochemical quality	No. of data points	Parameter value	Typical value	Value band width	No. of band widths from mean	Interpretation[2]
% residues in A, B, L	279	90.3	76.6	10.0	1.4	BETTER
Omega angle SD[1]	323	4.7	6.0	3.0	-0.4	Inside
Bad contact/100 residues	3	0.9	10.5	10.0	-1.0	Inside
Zeta angle SD	290	1.4	3.1	1.6	-1.1	BETTER
H-bond energy SD	218	0.7	0.9	0.2	-1.0	Inside
Overall G-factor	324	0.1	-0.6	0.3	2.3	BETTER

[1]SD denotes the standard deviation of the score observed, [2] – the accuracy of a structure (interpretation) is depicted in the order of Better > Inside > Worse for each parameter.

Table 1B. Summary of the side-chain parameters of SWISS-MODEL in Ramachandran plot

Stereochemical quality	No. of data points	Parameter value	Typical value	Value band width	No of band widths from mean	Interpretation[2]
Chi-1gauch minus SD[1]	39	12.0	22.7	6.5	-1.7	BETTER
Chi-1 trans SD	86	10.6	22.7	5.3	-2.3	BETTER
Chi-1 guache plus SD	129	12.4	21.3	4.9	-1.8	BETTER
Chi-1 pooled SD	254	12.0	22.0	4.8	-2.1	BETTER
Chi-2 trans SD	100	12.9	23.1	5.0	-2.0	BETTER

[1]SD denotes the standard deviation of the score observed, [2] – the accuracy of a structure (interpretation) is depicted in the order of Better > Inside > Worse for each parameter.

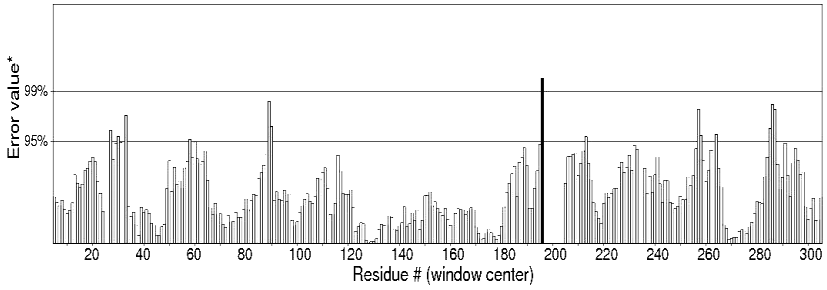

A)

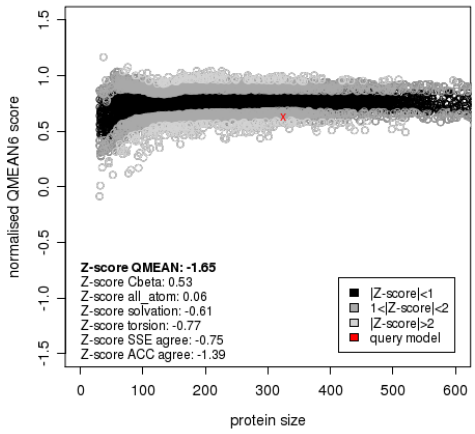

B)

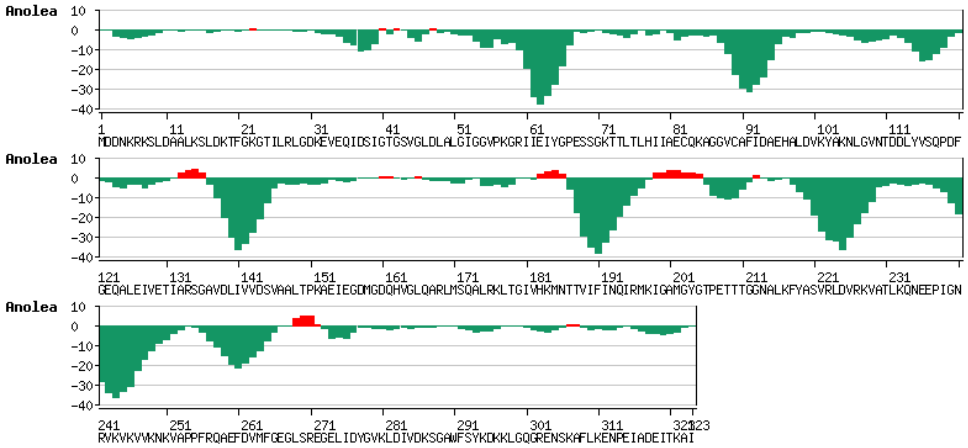

C)

Fig. 3 A) ERRAT results of *C. jejuni* RecA model produced by SWISS-MODEL. Black bars represent misfolded regions. On the error axis two lines are drawn to indicate the confidence with which it is possible to reject regions that exceed that error value;
B) ANOLEA plot of the non-local energy profile of the model predicted by SWISS-MODEL, high energy zones (red-colored) indicates more problematic areas;
C) QMEAN6 statistical potentials are normalized by Z-scores against non redundant set of known experimental structures.

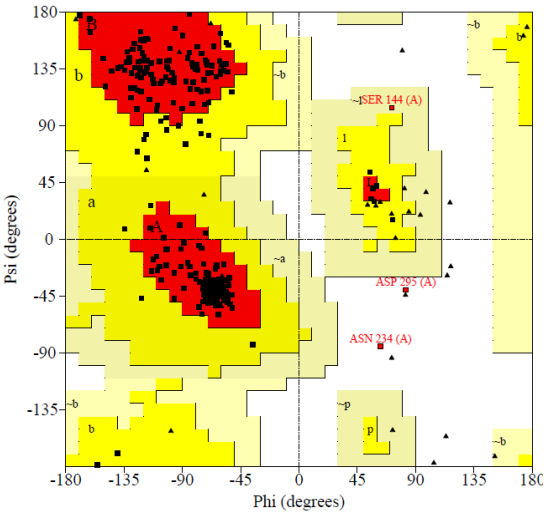

Fig. 4 Ramachandran plot of *C. jejuni* RecA by PROCHECK. The most favored regions are marked as A, B, and L (red-colored areas). The additional allowed regions are marked as a, b, l, and p, (yellow-colored areas). Residues in generously allowed regions as ~a,~b,~l,~p, (light-brown colored areas). All non-glycine and proline residues are shown as filled black squares where as glycines (non-end) are shown as filled black triangles. Disallowed amino acid residues are red-colored squares.

The FunFold tool predicted the active site of this protein for binding ADP/ATP. This area consists of Pro^{66}, Glu^{67}, Ser^{68}, Ser^{69}, Gly^{70}, Lys^{71} and Thr^{72}. RecA contains ATP binding motif of Walker-A type found in many bacterial proteins and have the conserved sequence GX4GK[S/T]. A variant of this motif, KGGXGK[S/T]T is involved in ATP hydrolysis and dimer formation [20, 43].

The results of docking are presented in Table 2. Each docking program places different weight on the energy terms exploited in calculations and various scoring systems are available, therefore, more than one tool is recommended to get more successful results. Quercetin (Figs. 5A and 6A) had the highest docking score in comparison to ADP. In a study of antimicrobial activity against Gram-positive and Gram-negative pathogens, Hirari et al. [17] found selective antibacterial properties of quercetin against methicillin-resistant *Staphylococcus aureus* (MRSA) and *S. epidermidis*. Quercetin induced the aggregation of *S. aureus* cells and significantly increased the antibacterial activity of oxacillin, ampicillin, vancomycin, gentamicin, and erythromycin against MRSA. Quercetin (3,5,7,3',4'-pentahydroxyflavone) and its analogues present in fruits, vegetables, leaves and grains were reported to possess anti-cancer protective activities by inhibiting inducible nitric oxide synthases that are expressed in human cancerous cells [32, 42].

It has been shown that the bioactivity of phenolic compounds is attributed to the presence of large number of hydroxyl groups. Thus, polyphenolic compounds can form large complexes with proteins and bacterial membranes [29, 46]. These polyphenolics are widely distributed in nature, e.g., taxifolin (5, 7, 3', 4'-tetrahydroxydihydroflavonol) is found in pericarp of tamarind, *Tamarindus indica* while vitexin (8-C-glucosylapigenin) can be extracted from fenugreek seeds [22, 37]. The most popular Indian spice, turmeric, obtained from *Curcuma longa*, contains curcumin (1,7-bis (4-hydroxy-3-methoxyprenyl)-1,6-heptadiene-3,5-dione) and two demethoxy compounds, demethoxy curcumin and bis-demethoxy curcumin that are diarylheptanoids. These compounds can inhibit many Gram-positive and Gram-negative

bacteria. Curcumin exhibited *in vitro* inhibition of *Staphylococcus aureus* at concentrations of 2.5-50 mg/100 ml [7].

Table 2. Docking results of *C. jejuni* RecA binding site with natural products

Compound	Database ID	Hex 8.0.0/ total interaction energy (Kcal/mol)	ArgusLab/ docking energy (Kcal/mol)	RecA residues involved in H-bonding
ADP	ZINC12368703	-268.23	-8.61	Ser^{68}, Ser^{69}, Gly^{70}, Lys^{71}, Thr^{72}, Thr^{73}, Tyr^{102}
Quercetin	ZINC03869685	-239.69	-10.34	Ser^{68}, Gly^{70}, Lys^{71}, Thr^{73}, Glu^{95}, Ala^{97}, Asp^{99}
Taxifolin	ZINC00105086	-352.74	-9.83	Ser^{68}, Ser^{69}, Gly^{70}, Lys^{71}, Thr^{72}, Thr^{73}, Ala^{97}, Asp^{99}
Vitexin	ZINC04349745	-289.28	-9.48	Ser^{68}, Thr^{72}, Glu^{95}, Asp^{99}, Asp^{143}
Catechin	ZINC00119983	-236.38	-9.43	Ser^{68}, Thr^{72}, Glu^{95}, Asp^{99}, Asp^{143}, Ser^{144}
Coumestrol	ZINC00001219	-215.20	-9.19	Ser^{68}, Gly^{70}, Thr^{73}, Asp^{99}, Tyr^{102}
Myricetin	ZINC03874317	-247.23	-9.09	Ser^{69}, Thr^{72}, Thr^{73}, Ala^{97}, Asn^{240}
Genkwanin	ZINC05732375	-263.31	-8.83	Ser^{68}, Thr^{72}, Glu^{95}, Asp^{99}, Tyr^{102}
Isoquercitrin	ZINC04096845	-293.83	-8.81	Ser^{68}, Gly^{70}, Lys^{71}, Thr^{72}, Thr^{73}, Ser^{144}
Epicatechin	ZINC00119988	-231.25	-8.74	Ser^{68}, Lys^{71}, Thr^{72}, Thr^{73}, Glu^{95}, Tyr^{102}, Asn^{240}
Cucurmin	ZINC31261437	-374.24	-8.66	Ser^{68}, Lys^{71}, Thr^{73}, Asn^{240}

Cucurmin (Fig. 5B), taxifolin (known as dihydroquercitin) (Fig. 5C), vitexin and isoquercitrin also had higher scores than ADP in Hex 8.0.0. These compounds (their structures are shown in Fig. 6) make hydrogen bonding with the same RecA residues involved in binding of ADP, see Fig. 7. Therefore, they may also interfere with their activities on RecA.

Table 3 presents the molecular properties of the flavonoids used. Lipinski et al. [26] devised a rule of five to describe the permeability of a candidate drug via oral route which is based on molecular weight (less than 500), H-bonds donors (less than 5), H-bond acceptors (less than 10) and logP (logarthim of octanol: water coefficient should be less than 5). In contrast to isoquercitrin, other compounds either had one or none violation. Quercetin, cucurmin and taxifolin do not exhibit any violation of this rule. Isoquercitrin had the highest values in respect to molecular weight, polar surface area, H-bond donors and acceptors, hence, it is not likely to be absorbed efficiently via oral route. The lipophilicity of an agent is measured by logP and is used to predict drug permeability [39]. de la Nuez and Rodríguez [14] stated that the relationship between logP and permeability is non-linear so it decreases at both low and high logP. The Polar surface area (PSA) is widely used to predict intestinal absorption of molecules. Several studies found an experimental correlation between PSA and the permeability through CACO-2 cells. Poor intestinal absorption is likely to occur if a drug has PSA greater than 140 $Å^2$ [30, 41].

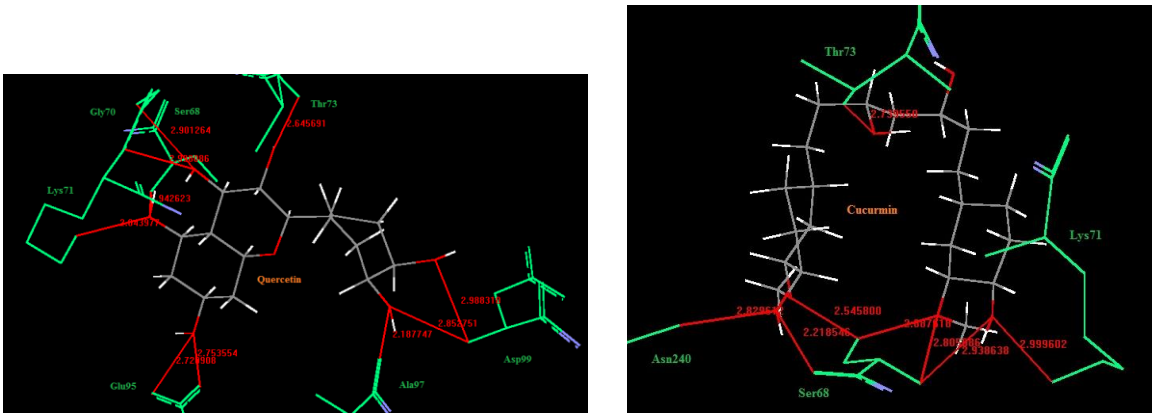

A) B)

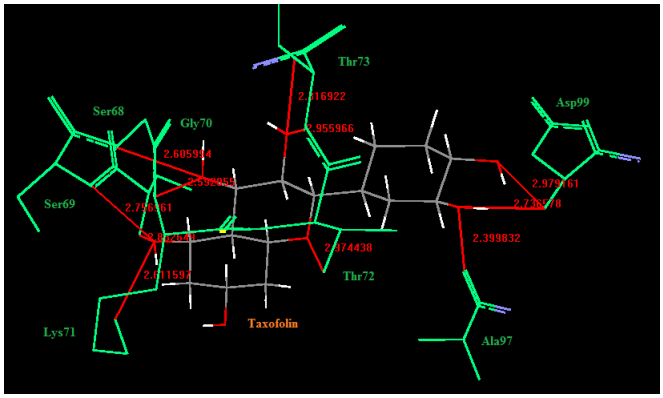

C)

Fig. 5 Interaction of flavonoids at ATP-binding site:
A) Quercetin forms H-bonds with the residues Ser^{68} (2.942 Å), Gly^{70} (2.901 Å), Lys^{71} (2.643 and 2.998 Å), Thr^{73} (2.645), Ala^{97} (2.187 Å) and Asp^{99} (2.988 and 2.852 Å); (B) Cucurmin forms H-bonds with the residues Ser^{68} (2.218, 2.545, 2.805, 2.687 and 2.938 Å), Lys^{71} (2.999 Å), Thr^{73} (2.739 Å) and Asn^{240} (2.829 Å); (C) Taxifolin forms H-bonds with the residues Ser^{68} (2.882 Å), Ser^{68} (2.756 Å), Gly^{70} (2.605 and 2.599 Å), Lys^{71} (2.611 and 2.592 Å), Thr^{72} (2.974 Å), Thr^{73} (2.316 and 2.955 Å), Ala^{97} (2.399 Å) and Asp^{99} (2.971 and 2.736 Å). H-bonds are red colored (numbers refer to distances) whereas amino acids are green. Viewed by ArgusLab 4.0.1 [40].

Table 3. Physiological properties of the compounds

Compound	Weight, (g/mol)	logP	H-bond donors	H-bond acceptors	Polar surface area, (Å)
Quercetin	302.24	1.68	5	7	131
Taxifolin	288.26	0.71	2	7	127
Vitexin	432.38	0.52	7	10	181
Catechin	290.27	1.68	5	6	110
Coumestrol	268.22	2.54	2	5	84
Myricetin	318.24	1.39	6	8	152
Genkwanin	284.27	3.00	2	5	80
Isoquercitrin	464.38	-0.36	8	12	211
Epicatechin	290.27	1.37	5	6	110
Cucurmin	368.39	2.30	2	6	93

Polysulfated naphthyl compounds and ATP nucleotide analogs were also found to be inhibitors of RecA *in vitro* [45]. To search for small molecules that can inhibit nucleoprotein filament assembly between RecA and DNA strands, Sexton et al. [36] screened a library of 33,600 compounds. ATPase test was carried out to measure activity and 40 compounds were selected to be inhibitors. The most potent inhibitors were 2-amino-4,6-diarylpyridines in micromolar ranges. N(6)-(1-naphthyl)-ADP was also used to inhibit *E. coli* RecA ATP binding site in a study to suppress dissemination of antibiotic resistance [25]. However, these compounds did not show such an activity in bacterial cultures [36].

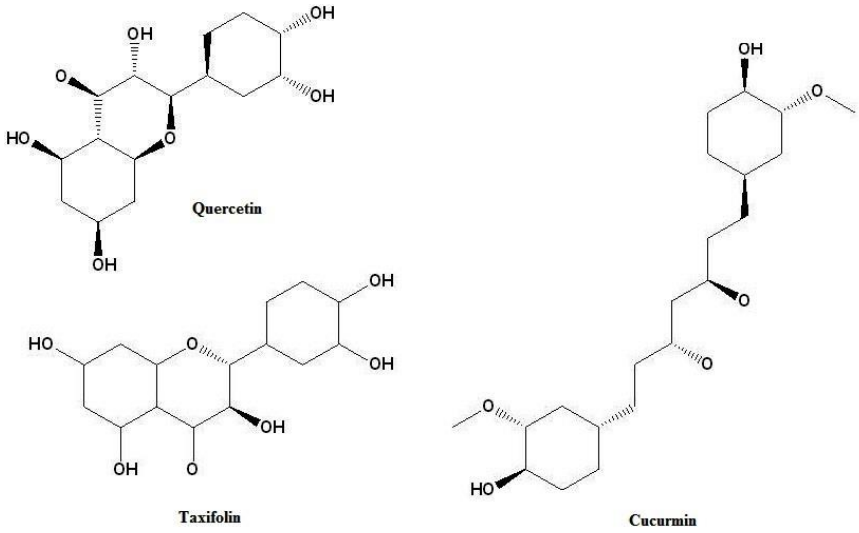

Fig. 6 Chemical structures of the natural products having the highest docking scores in ArgusLab 4.0.1 and Hex 8.0.0.

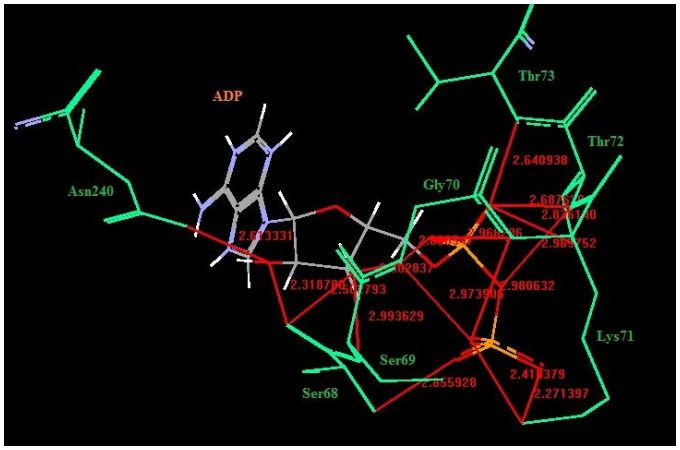

Fig. 7 Interaction of ADP at binding site. ADP forms fourteen H-bonds with the residues Ser^{68} (2.318 and 2.855 Å), Gly^{70} (2.802, 2.600 and 2.973 Å), Lys^{71} (2.410, 2.227, 2.687, 2.965, 2.966 and 2.980 Å), Thr^{72} (2.640, 2.687, 2.836 and 2.965 Å), Thr^{73} (2.640 Å), Asn^{240} (2.613 Å). H-bonds are red colored (numbers refer to distances whereas amino acids are green. Viewed by ArgusLab 4.0.1 [40].

In silico methods for drug design assist in the identification of drug targets using various bioinformatics tools. They can also be used to analyze the target for binding sites and dock particular compounds with the target, rank them according to their binding affinities and

obtain lead compounds for drug discovery. As the structural information of many protein targets become available, there is an increasing demand for computer based tools since they are free and or have low costs [16].

Conclusion

Although natural compounds provide a good source for providing antimicrobials, optimization of a lead compound may be required to improve its pharmacokinetics and efficacy inside human body, e.g., adding a methyl group to enhance the lypophilic property which results in 0.6 Kcal/mol improvement in binding active site [1]. A candidate antibiotic should not affect human body. It should target an essential function of microorganisms such as DNA recombination and repair induced by antibiotic exposure.

References

1. Andrews P. R., D. J. Craik, J. L. Martin (1984). Functional Group Contributions to Drug-receptor Interactions, J Med Chem, 27, 1648-1657.
2. Arnold K., L. Bordoli, J. Kopp, T. Schwede (2006). The Swiss-model Workspace: A Web-based Environment for Protein Structure Homology Modeling, Bioinformatics, 22, 195-201.
3. Balajee R., Dr. M. S. Dhana Rajan (2011). Molecular Docking Studies of Pantothenate Synthase Bound with Novel Molecules for *Mycobacterium tuberculosis*, J Pharm Sci Res, 3(6), 1276-1279.
4. Beaber J. W., B. Hochhut, M. K. Waldor (2004). SOS Response Promotes Horizontal Dissemination of Antibiotic Resistance Genes, Nature, 427(6969), 72-74.
5. Benkert P., M. Biasini, T. Schwede (2011). Toward the Estimation of the Absolute Quality of Individual Protein Structure Models, Bioinformatics, 27(3), 343-350.
6. Benkert P., M. Kunzli, T. Schwede (2009). QMEAN Server for Protein Model Quality Estimation, Nucleic Acids Res, 37, W510-W514.
7. Bhavani Shankar T. N., V. Srinivasamurthy (1979). Effect of Turmeric Fractions on the Growth of Some Intestinal and Pathogenic Bacteria *in vitro*, Indian J Experi Biol, 17, 1363-1366.
8. Castrignano T., P. D. De Meo, D. Cozzetto, I. G. Talamo, A. Tramontano (2006). The PMDB Protein Model Database, Nucleic Acids Res, 34(1), D306-D309.
9. Chen Z., H. Young, N. P. Pavletich (2008). Mechanism of Homologous Recombination from the RecA-ssDNA/dsDNA Structures, Nature, 453, 489-494.
10. Cheng J., A. Randall, M. Sweredoski, P. Baldi (2005). SCRATCH: A Protein Structure and Structural Feature Prediction Server, Nucleic Acids Res, 33, W72-W76.
11. Chikhi A., A. Bensegueni (2008). Docking Efficiency Comparison of Surflex, A Commercial Package and Arguslab, A Licensable Freeware, J Comput Sci Syst Biol, 1, 81-86.
12. Colovos C., Y. O. Yeates (1993). Verification of Protein Structures: Patterns of Non-bonded Atomic Interactions, Protein Sci, 2, 1511-1519.
13. Cox M. M. (2007). Regulation of Bacterial RecA Protein Function, Crit Rev Biochem Mol Biol, 42, 41-63.
14. de la Nuez A., R. Rodríguez (2008). Current Methodology for the Assessment of ADME-tox Properties on Drug Candidate Molecules, Biotec Aplicada, 25(2), 97-110.
15. Džidić S., J. Šušković, B. Kos (2008). Antibiotic Resistance in Bacteria, Food Technol Biotechnol, 46(1), 11-21.
16. Gupta K., A. Kumar (2016). Open Tools of Drug Designing for Open Research, Int J Bioautomation, 20(2), 159-182.

17. Hirai I., M. Okuno, R. Katsuma, N. Arita, M. Tachibana, Y. Yamamoto (2010). Characterisation of anti-*Staphylococcus aureus* Activity of Quercetin, Inter J Food Sci Technol, 45(6), 1250-1254.
18. Irwin J. J., T. Sterling, M. M. Michael, E. S. Bolstad, R. G. Coleman (2012). ZINC: A Free Tool to Discover Chemistry for Biology, J Chem Inf Model, 52, 1757-1768.
19. Kabsch W., C. Sander (1983). Dictionary of Protein Secondary Structure: Pattern Recognition of Hydrogen-bonded and Geometrical Features, Biopolymers, 22(12), 2577-2637.
20. Koonin E. V. (1993). A Superfamily of Atpases with Diverse Functions Containing Either Classical or Deviant ATP-binding Motif, J Mol Biol, 229, 1165-1174.
21. Kowalczykowski S. C. (1991). Biochemical and Biological Function of *Escherichia coli* RecA Protein: Behavior of Mutant RecA Proteins, Biochimie, 73, 289-304.
22. Krishnamurthy K. S., V. P. Sapna, V. A. Parthasarathy (2008). Tamarind, In: Chemistry of Spices, Parthasarathy V. A., B. Chempakam, T. J. Zachariah, Eds., CAB International, Cambridge, 362-375.
23. Laskowski R. A., M. W. MacArthur, D. Moss, J. M. Thornton (1993). Procheck: A Program to Check the Stereochemical Quality of Protein Structures, J Appl Crystal, 26(2), 283-291.
24. Lazaridis T., M. Karplus (2000). Effective Energy Functions for Protein Structure Prediction, Curr Opin Struct Biol, 10, 139-145.
25. Lee A. M., C. T. Ross., B. B. Zeng, S. F. Singleton (2005). A Molecular Target for Suppression of the Evolution of Antibiotic Resistance: Inhibition of the *Escherichia coli* RecA Protein by N (6)-(1-naphthyl)-ADP, J Med Chem, 8(17), 5408-5411.
26. Lipinski C. A., F. Lombardo, B. W. Dominy, P. J. Feeney (2001). Experimental and Computational Approaches to Estimate Solubility and Permeability in Drug Discovery and Development Settings, Adv Drug Deliv Rev, 46, 3-26.
27. Melo F., D. Devos, E. Depiereux, E. Feytmans (1997). ANOLEA: A WWW Server to Assess Protein Structures, Proc Int Conf Intell Syst Mol Biol, 5, 187-190.
28. Modi V., N. Mathur, A. N. Pathak (2013). Molecular Docking Studies of Anti-HIV Drug BMS-488043 Derivatives Using HEX and GP 120 Interaction Analysis Using Pymol, Int J Sci Res Pub, 3(6), 1-7.
29. Mueller-Harvey I., A. B. McAllan (1992). Tannins: Their Biochemistry and Nutritional Properties, adv Plant Cell Biochem Biotechnol, 1, 151-217.
30. Pajouhesh H., G. R. Lenz (2005). Medicinal Chemical Properties of Successful Central Nervous System Drugs, NeuroRx, 2(4), 541-553.
31. Ramachandran G. N., V. Sasisekharan (1968). Conformation of Polypeptides and Proteins, Adv Protein Chem, 23, 283-437.
32. Raso G. M., R. Meli, G. Di Carlo, M. Pacilio, R. Di Carlo (2001). Inhibition of Inducible Nitric Oxide Synthase and Cyclooxygenase-2 Expression by Flavonoids in Macrophage J774A.1, Life Sci, 68, 921-931.
33. Ritchie D. W., V. Venkatraman (2010). Ultra-fast FFT Protein Docking on Graphics Processors, Struct Bioinformatics, 26(19), 2398-2405.
34. Roche D. B., S. J. Tetchner, L. J. McGuffin (2011). FunFOLD: An Improved Automated Method for the Prediction of Ligand Binding Residues Using 3D Models of Proteins, BMC Bioinformatics, 12, 160.
35. Sassanfar M., J. W. Roberts (1990). Nature of the SOS-inducing Signal in *Escherichia coli*: The Involvement of DNA Replication, J Mol Biol, 212(1), 79-96.
36. Sexton J. Z., T. J. Wigle., Q. He, M. Hughes, G. R. Smith, S. F. Singleton, A. L. Williams, L. Yeh (2010). Novel Inhibitors of *E. coli* RecA ATPase Activity, Curr Chem Genom, 4, 34-42.

37. Shang M., S. Cai, J. Han, J. Li, Y. Zhao, J. Zheng, T. Namba, S. Kadota, Y. Tezuka, W. Fan (1998). Studies on Flavonoids from Fenugreek (*Trigonella foenum-graecum*). China J Chinese Materia Medica, 23(10), 614-616.
38. Sindhu T., S. Rajamanikandan, D. Durgapriya, J. R. Anitha, S. Akila, V. K. Gopalakrishnan (2011). Molecular Docking and QSAR Studies on Plant Derived Bioactive Compounds as Potent Inhibitors of DEK Oncoprotein, Asian J Pharmaceutical Clin Res, 4(2), 67-71.
39. Testa B., P. A. Carrupt, P. Gaillard, F. Billois, P. Weber (1996). Lipophilicity in Molecular Modelling, Pharm Res, 13, 335-343.
40. Thompson M. A. (2004). Molecular Docking Using Arguslab, an Efficient Shape-based Search Algorthim and Score Based Search Algortithm and the Ascore Scoring Function, ACS Meeting, Philadelphia 172 CINF 42 PA.
41. Van de Waterbeemd H., G. Camenisch, G. Folkers, O. A. Raevsky (1996). Estimation of CACO-2 Cell Permeability Using Calculated Molecular Descriptors, Quant Struct-Act Relat, 15, 480-490.
42. Verschoyle R. D., W. P. Steward, A. J. Gescher (2007). Putative Cancer Chemopreventive Agents of Dietary Origin-how Safe are They, Nature, 59, 152-162.
43. Walker J. E., M. Saraste, M. J. Runswick, N. J. Gay (1982). Distantly Related Sequences in the Alpha- and Beta-subunits of ATP Synthase, Myosin, Kinases and Other ATP-requiring Enzymes and a Common Nucleotide Binding Fold, EMBO J, 1, 945-951.
44. Wang R., L. Lai, S. Wang (2002). Further Development and Validation of Empirical Scoring Functions for Structure-based Binding Affinity Prediction, J Comp Aided Mol Design, 16, 11-26.
45. Wigle T. J., S. F. Singleton (2007). Directed Molecular Screening for RecA ATPase Inhibitors, Bioorg Med Chem Lett, 17(12), 3249-3253.
46. Zongo C., A. Savadogo, K. M. Somda, J. Koudou, A. S. Traore (2011). *In vitro* Evaluation of the Antimicrobial and Antioxidant Properties of Extracts from Whole Plant of *Alternanthera pungens* H. B. and K. & Leaves of *Combretum sericeum* G. Don, Int J Phytomedicine, 3, 182-191.

Mohammed Zaghlool Al-Khayyat
E-mail: mzsaeed19@hotmail.com

Mohammed Zaghlool Al-Khayyat was born on August 19, 1972 in Baghdad, Iraq. Currently he is a lecturer of the Practical Lab Genetics, Biology Department, College of Science, University of Mosul, Iraq.